Bioprocess and Biosystems Engineering (2020) 43:373–381
https://doi.org/10.1007/s00449-019-02233-3

RESEARCH PAPER

Modification of carbon felt anode with graphene/Fe_2O_3 composite for enhancing the performance of microbial fuel cell

Lin Fu[1,2] · Haoqi Wang[1,2] · Qiong Huang[3] · Tian-shun Song[1,2,3] · Jingjing Xie[1,2,4]

Received: 19 June 2019 / Accepted: 14 October 2019 / Published online: 28 October 2019

Abstract
In this paper, a graphene/Fe_2O_3 (G/Fe_2O_3) modified anode was prepared through a simple one-step hydrothermal reduction method to improve the performance of microbial fuel cell (MFC). The power density of MFC with the G/Fe_2O_3 anode was 334 ± 4 mW/m^2, which was 1.72 times and 2.59 times that of MFC with a graphene anode and an unmodified anode, respectively. Scanning electron microscopy and iron reduction rate experiment showed that G/Fe_2O_3 materials had good biocompatibility. Furthermore, microbial community analysis results indicated that the predominant populations on the anode biofilm belonged to *Enterobacteriaceae*, and the abundance of *Desulfovibrio* increased in the presence of the Fe_2O_3. Thus, the combination of graphene and Fe_2O_3 provided high electrical conductivity to facilitate extracellular electron transfer (EET) and improved biocompatibility to promote the cable bacteria formation and enhance electron transport efficiency over long distances. Therefore, G/Fe_2O_3 is an effective anode material for enhancing the performance of MFCs.

Keywords Microbial fuel cell · Graphene · Fe_2O_3 · Microbial community · Electricity generation

Introduction

Microbial fuel cells (MFCs) represent a green energy conversion technology [1]. In MFCs, exoelectrogenic bacteria are used to recover the chemical energy stored in biodegradable organic materials for conversion into electrical energy [2]. They have great potential for simultaneously addressing the needs for energy regeneration and organic waste treatment [3]. Electrons are transferred through an anode and passed through an external circuit to reach a cathode. Protons released from the substrates diffuse across an ion exchange membrane into a cathode compartment where they subsequently combine with the final electron acceptor, such as molecular oxygen, to form water; circuit and electricity generation are completed via the redox reaction process [4, 5]. Therefore, efficient extracellular electron transfer (EET) at the anode is crucial in MFCs. EET can be affected by the type and composition of anode materials [6]. Carbon felt (CF) [7], carbon cloth (CC) [8], and carbon paper (CP) [9] are commonly used as anode materials because they are relatively stable and have good electrical conductivity. Graphene has a large specific surface area, high electronic conductivity, and excellent mechanical strength [10, 11], so it can be used to modify electrodes and improve MFC performance [12]. However, it has been reported that electrochemically active bacteria and graphene are negatively charged; consequently, an electrostatic repulsion can be generated between the bacteria and graphene. This phenomenon leads to a lower number of bacteria attached on the graphene surface, which eventually ceases the bacterial growth [13].

✉ Tian-shun Song
tshsong@njtech.edu.cn

✉ Jingjing Xie
xiej@njtech.edu.cn

[1] State Key Laboratory of Materials-Oriented Chemical Engineering, Nanjing Tech University, Nanjing 211816, People's Republic of China

[2] College of Biotechnology and Pharmaceutical Engineering, Nanjing Tech University, Nanjing 211816, People's Republic of China

[3] Jiangsu Collaborative Innovation Center of Atmospheric Environment and Equipment Technology, Jiangsu Key Laboratory of Atmospheric Environment Monitoring and Pollution Control (AEMPC), Nanjing University of Information Science and Technology, Nanjing 210044, People's Republic of China

[4] Jiangsu National Synergetic Innovation Center for Advanced Materials (SICAM), Nanjing 211816, People's Republic of China

Molecular simulations and a series of experiments have revealed the behavior of electron transfer from the OM c-Cyts to minerals containing Fe (III) in vitro and in vivo [14, 15]. Therefore, MFC performance has been improved through the addition of ferric iron [16]. The insoluble metal Fe_2O_3, a bioavailable Fe (III) oxide, has high affinity for C-type dehydrated cytochromes (OmcA and MtrC) on the outer membrane of the *Shewanella* species [17], and enhances electrical output and increases maximum power density [15, 18]. However, the poor conductivity of Fe_2O_3 limits the further improvement of MFC performance. Thus, the effective combination of graphene with good electronic conductivity and Fe_2O_3 with good biocompatibility can provide advantages and improve the performance of MFC.

In this study, graphene/Fe_2O_3 (G/Fe_2O_3) materials were used to modify the anode through solvothermal reduction method. MFCs with graphene and unmodified anode were used as control. Material characteristics were determined through scanning electron microscopy (SEM), transmission electron microscopy (TEM), and X-ray diffraction (XRD). The electrochemical capabilities of different anodes were also characterized through cyclic voltammetry (CV). The microbial community structures of the anode biofilms in MFCs were further analyzed by employing Illumina high-throughput sequencing.

Materials and methods

Electrode preparation

CF was immersed in 1 mol L^{-1} HCl and 1 mol L^{-1} NaOH for 24 h to remove metal impurities and organics, respectively. Then, CF was washed several times with deionized water to ensure that its surface was clean. The G/Fe_2O_3 preparation method was based on the report of Jin et al. [19]. Briefly, 200 mg of graphene oxide (GO) (Hunan Fenghua Material Development Co., Ltd.) was added to 80 mL of ethylene glycol (EG) solution and sonicated for 20 min. $FeCl_3$ (200 mg) was then added to the homogeneous GO solution for 20 min of sonication. Sodium acetate (3.04 g) was added to the solution and stirred for 1 h. CF (5 cm × 5 cm, 25 cm^2) was transferred to a Teflon autoclave with the above solution and refluxed in the autoclave at 200 °C for 24 h, and finally cooled to room temperature. The G/Fe_2O_3–CF was washed with deionized water and dried at 80 °C. G–CF was also prepared through the same procedures in the absence of $FeCl_3$.

MFC setup and operation

The glass dual-chamber reactor with an effective volume of 250 mL for anode and cathode chambers was used. A proton exchange membrane (Nafion 117; Dupont Co., USA) was selected to separate the anode and cathode chambers. A CF (5 cm × 5 cm, 25 cm^2) was used as the cathode in all the reactors. CF, G/Fe_2O_3–CF and G–CF were used as the anodes of the MFCs. The anodic chamber was inoculated with the local anaerobically fermented biomass sludge. The anolyte contained 0.31 g/L NH_4Cl, 11.53 g/L $Na_2HPO_4 \cdot 12H_2O$, 2.77 g/L $NaH_2PO_4 \cdot 2H_2O$, 0.13 g/L KCl, and 2 g/L glucose. The catholyte consisted of 13.2 g/L $K_3[Fe (CN)_6]$, 11.53 g/L $Na_2HPO_4 \cdot 12H_2O$, 2.77 g/L $NaH_2PO_4 \cdot 2H_2O$ and 0.13 g/L KCl. The MFCs were operated at a 1000 Ω and performed in duplicate at 28 ℃.

Iron reduction rate measurement

Iron reduction rate (FER) was measured on the basis of previous reports [20]. The nutrient solution consisted of (per liter of deionized water): 2.5 g $NaHCO_3$, 0.1 g KCl, 0.6 g $NaH_2PO_4 \cdot 2H_2O$, 1.5 g NH_4Cl, 2.2 g glucose and 7.3 g ferric citrate. The sterilized nutrient solution was distributed into a 100 mL anaerobic bottle (effective volume of 40 mL per bottle). Oxygen was removed by blowing pure N_2 for 10 min to create an anaerobic environment. At the end of the experiment, the anode was taken out and vortex oscillation was performed in distilled water to obtain a bacterial suspension. Next, 5% (V/V) of the bacterial suspension was inoculated to anaerobic bottle and incubated at 28 °C. The samples were taken every 12 h. Ferrous content was analyzed and measured with the phenanthroline method [21].

Analytical method

The crystal structures of the samples were investigated by X-ray diffraction (XRD; Rigaku Smartlab 3 kW) using a Cu-Kα radiation source ranging from 5° to 80° at a scan rate of 10° min^{-1}. The morphological characteristics of G/Fe_2O_3 were analyzed by transmission electron microscopy (JEM-2100F, Japan). The surface morphologies of the anodes were investigated by SEM and coupled energy dispersive spectroscopy (SEM–EDS; JSM-5900, Japan). Voltages were continuously monitored using a precision multimeter and a data acquisition system (Keithley Instruments 2700, USA). Polarization curve and output power curves were then constructed by discharging the cell with external resistor values from 50 to 5000 Ω [22]. Internal resistance was calculated by the polarization slope method. CV was performed on a potentiostat (CHI660E Chenhua Instrument Co., China) in a three-electrode configuration. The test range was − 1000 to 200 mV and the scan rate was 10 mV/s. The anode was used as the working electrode, while the cathode and Ag/AgCl was used as the counter and the reference electrodes, respectively. Genomic DNA was extracted using Power Soil®DNA Isolation Kit (MO BIO Laboratories Inc., Carlsbad, CA, USA) in accordance with the manufacturer's protocol. Illumina high-throughput sequencing was performed by Majorbio (Shanghai, China).

Results and discussion

Characterizations

The crystal structure of G/Fe_2O_3 was characterized by XRD (Fig. 1a). The characteristic peaks were found at $2\theta = 33.2°$, 35.6°, 40.9°, 49.5°, 54.1°, 57.4°, 62.4°, 64.0° and 75.4° corresponded to Fe_2O_3 crystals (JCPDS, No.33–664). Graphene showed a hump-shaped peak at 24.1°, which originated from the (002) diffraction [23]. This result indicated that Fe_2O_3 nanoparticles were successfully loaded onto graphene. Raman spectroscopy was also performed to investigate the carbon structure of G/Fe_2O_3 (Fig. 1b). The Raman spectrum of GO showed two main characteristic peaks at 1350 cm^{-1} and 1606 cm^{-1} that corresponded to the D band and the G band, respectively. The D band and G bands of G/Fe_2O_3 were also observed in Raman spectroscopy. The intensity of the D band was strongly associated with the breathing mode of the k-point phonon and the G band was attributed to the E_{2g} phonon from sp^2 carbon atom [24, 25]. In comparison with the intensity ratio (I_D/I_G) of GO, I_D/I_G of the G/Fe_2O_3 composite increased from 0.85 to 1.12; this increase demonstrated the successful reduction of GO and the formatting of multilayer graphene sheets by hydrothermal process [26]. The TEM image (Fig. 2a) showed that the Fe_2O_3 microspheres with a diameter of approximately 20 nm were closely packed in a thin wrinkle "paper-like" group of graphene nanosheets; this observation was consistent with previous reports [27]. It can be seen from the SEM image that the fiber of bare CF (Fig. 2b) was smooth. The rumpled graphene exhibited the typical structure of aggregated and stacked sheets on the G–CF fibers (Fig. 2c), while the aggregation tendency of graphene weakened in the presence of Fe_2O_3 (Fig. 2d). In addition, G/Fe_2O_3 and graphene were successfully loaded on the CF in Fig. 2.

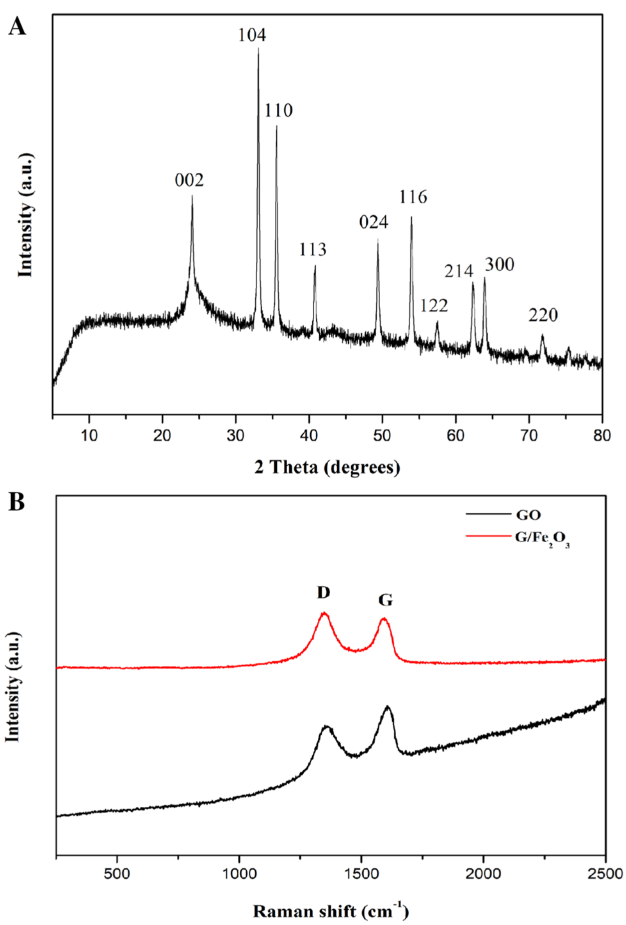

Fig. 1 **a** XRD pattern of G/Fe_2O_3 and **b** Raman spectra of GO and G/Fe_2O_3

MFC performance

Three reproducible voltage cycles were obtained in all MFCs (Fig. 3). The voltage of MFCs rapidly increased upon the replacement of the fresh culture media, remained steady value for a period time, and gradually decreased because of substrate depletion in all the MFCs. The MFC with G/Fe_2O_3–CF achieved a maximum stable voltage of 590 ± 5 mV, whereas the MFCs with G–CF and CF had maximum stable voltages of 555 ± 6 mV and 490 ± 6 mV, respectively.

The maximum power density (P_{max}) and polarization curves of the different MFCs were determined after 2 days of experimentation (Fig. 4). The slope of the polarization curve reflected the internal resistance of the MFCs (Table 1). The MFC with G/Fe_2O_3–CF generated the highest P_{max} of 334 ± 4 mW/m^2, followed by that of the MFC with G-CF (194 ± 3 mW/m^2). The MFC with CF (129 ± 4 mW/m^2) generated the lowest P_{max}. The P_{max} of MFC with G/Fe_2O_3-CF was 1.72 and 2.59 times that of the G-CF and CF. Internal resistance was calculated on the basis of the polarization curve. The lowest internal resistance (320 ± 5 Ω) was observed in the G/Fe_2O_3–CF group, followed by the MFC with G–CF (600 ± 4 Ω), while the MFC with CF had the highest internal resistance (666 ± 6 Ω). The internal resistance of the MFC with CF was 1.11 times and 2.08 times that of the MFCs with G–CF and the G/Fe_2O_3–CF, respectively. These results showed that the G/Fe_2O_3–CF successfully increased the output power and reduced the internal resistance of the MFCs.

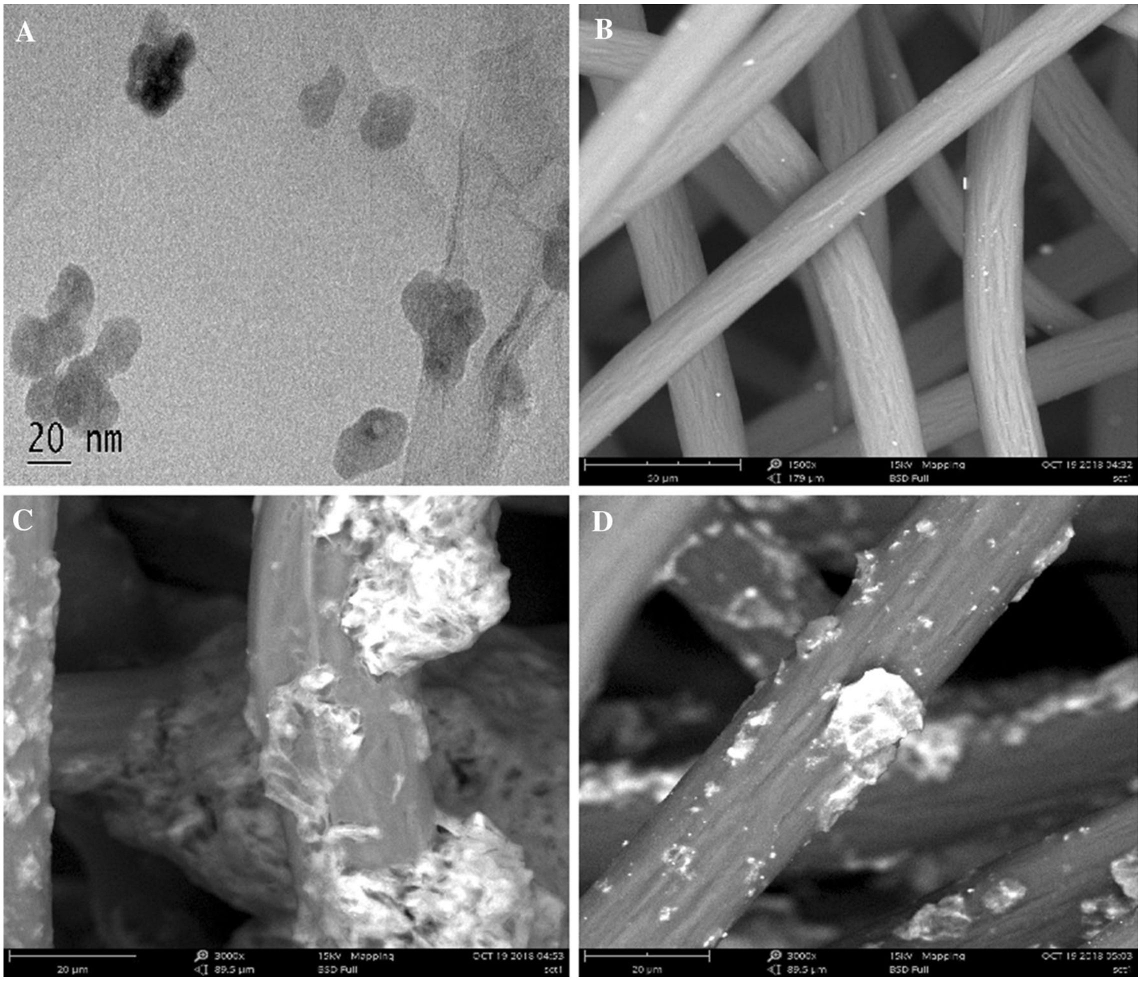

Fig. 2 TEM images of **a** G/Fe_2O_3 and SEM images of **b** CF **c** G-CF, and **d** G/Fe_2O_3-CF

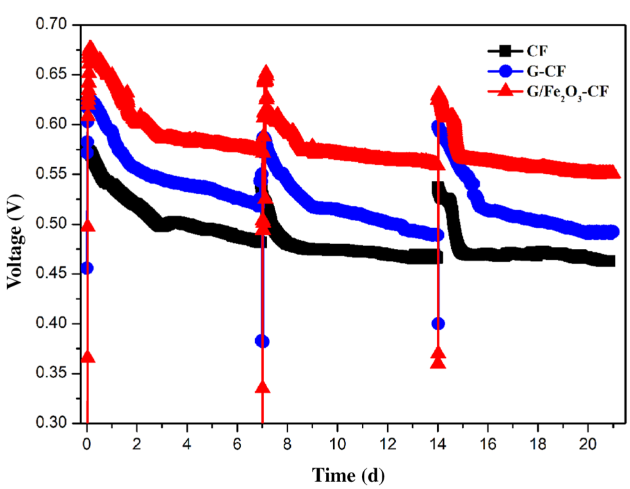

Fig. 3 Voltages of MFCs with CF, G-CF, and G/Fe_2O_3-CF over three cycles

Electrochemical characterization

CV measurements (Fig. 5) were conducted in the MFC reactor during a steady voltage period to study the electrochemical behavior of the anode. The maximum visible current of the positive (3.8 mA) and reverse (– 4.8 mA) scans of the CF anode was lower than that of the G–CF bioanode (6.2 mA and – 6.3 mA) likely because of the high electrical conductivity of graphene. The MFC with the G/Fe_2O_3–CF showed the highest anodic current (10.6 mA and – 12.4 mA). This result indicated that Fe_2O_3 was also beneficial to the improvement of the electron transfer capability of the anode.

Iron reduction rate

During the first 24 h of incubation, Fe (II) concentration accumulated slowly in all groups (Fig. 6). The rapid increase in Fe (II) concentration during a later period might be due to microbial growth and enrichment in the first 24 h. The

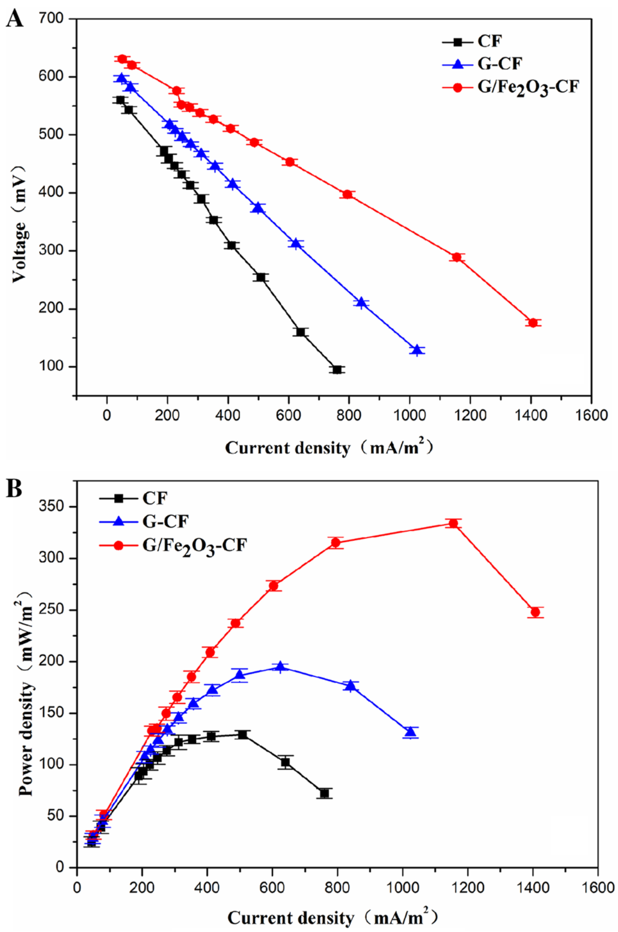

Fig. 4 **a** Polarization curve and **b** output power of MFCs with CF, G-CF, and G/Fe_2O_3-CF

Table 1 Comparison of the parameters of MFCs with different anode materials

Anode	Maximum stable voltage (mV)	Internal resistance (Ω)	Power density (mW/m^2)
CF	490 ± 6	666 ± 6	129 ± 4
G–CF	555 ± 6	600 ± 4	194 ± 3
G/Fe_2O_3–CF	590 ± 5	320 ± 5	334 ± 4

cumulative Fe (II) concentrations in G–CF and CF were significantly lower than that in the G/Fe_2O_3–CF in 72 h. The FER of the G/Fe_2O_3–CF was 3.04 ± 0.1 mg L^{-1} h^{-1}, whereas the FER of the of G–CF and CF groups was 1.80 ± 0.1 mg L^{-1} h^{-1} and 1.69 ± 0.15 mg L^{-1} h^{-1}, respectively. The highest FER was obtained by the microorganisms in G/Fe_2O_3–CF. The FER reflects the ability of microorganisms to transfer electrons [21]. The results also demonstrated that G/Fe_2O_3–CF was beneficial to the enhancement of the electron transfer of the MFC system.

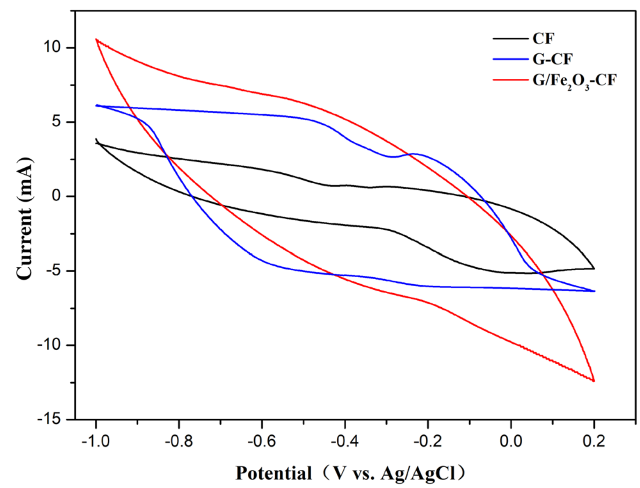

Fig. 5 Cyclic voltammetry curves of MFCs with CF, G-CF, and G/Fe2O3-CF

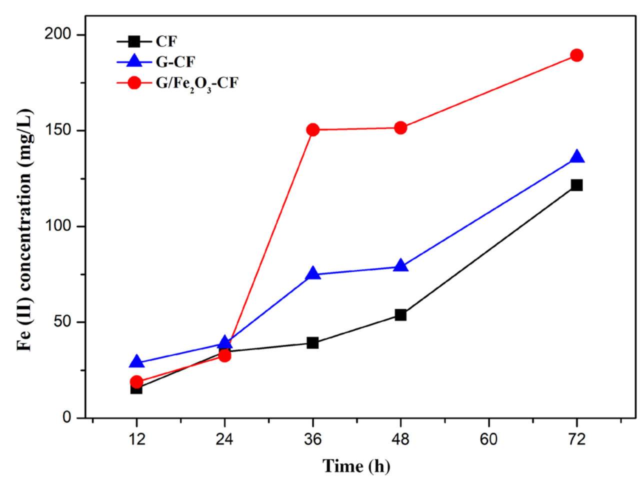

Fig. 6 The accumulation of Fe (II) with bacteria from CF, G-CF, and G/Fe_2O_3-CF

Bacterial community structure of biofilms in MFCs

The surfaces of the biofilms were analyzed by SEM at the end of the experiment (Fig. 7). The biofilm on CF was loose, the biofilm on G–CF thickened, and the biofilm on G/Fe_2O_3–CF was dense likely because of the good conductivity and biocompatibility in the presence of graphene and Fe_2O_3. Therefore, the affinity between the microorganisms and the anode could be enhanced.

The microbial communities in biofilms on different MFCs were analyzed at the end of the experiment. At the level of the phylum (Fig. 8a), Proteobacteria was the most abundant phylum in the microbial communities in all of the groups. The second-most abundant phylum was Firmicutes, followed by Bacteroidetes. The relative abundances of

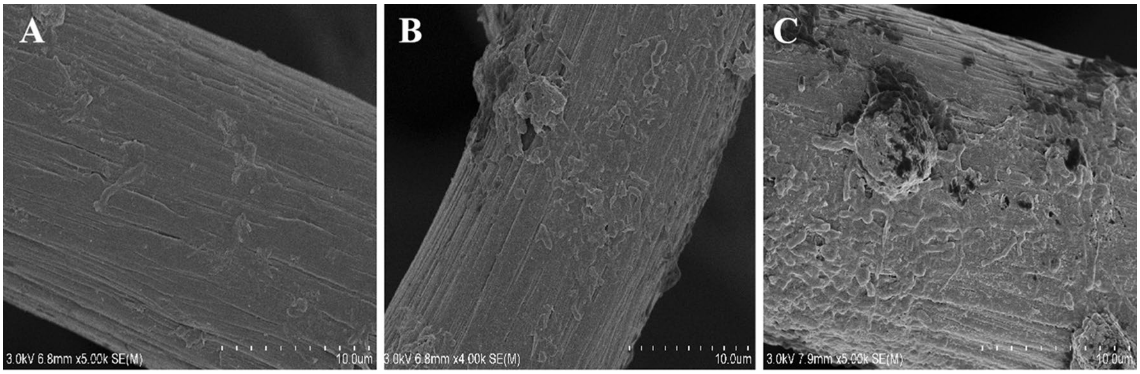

Fig. 7 SEM images of biofilms in **a** CF **b** G-CF, and **c** G/Fe_2O_3-CF at the end of the experiment

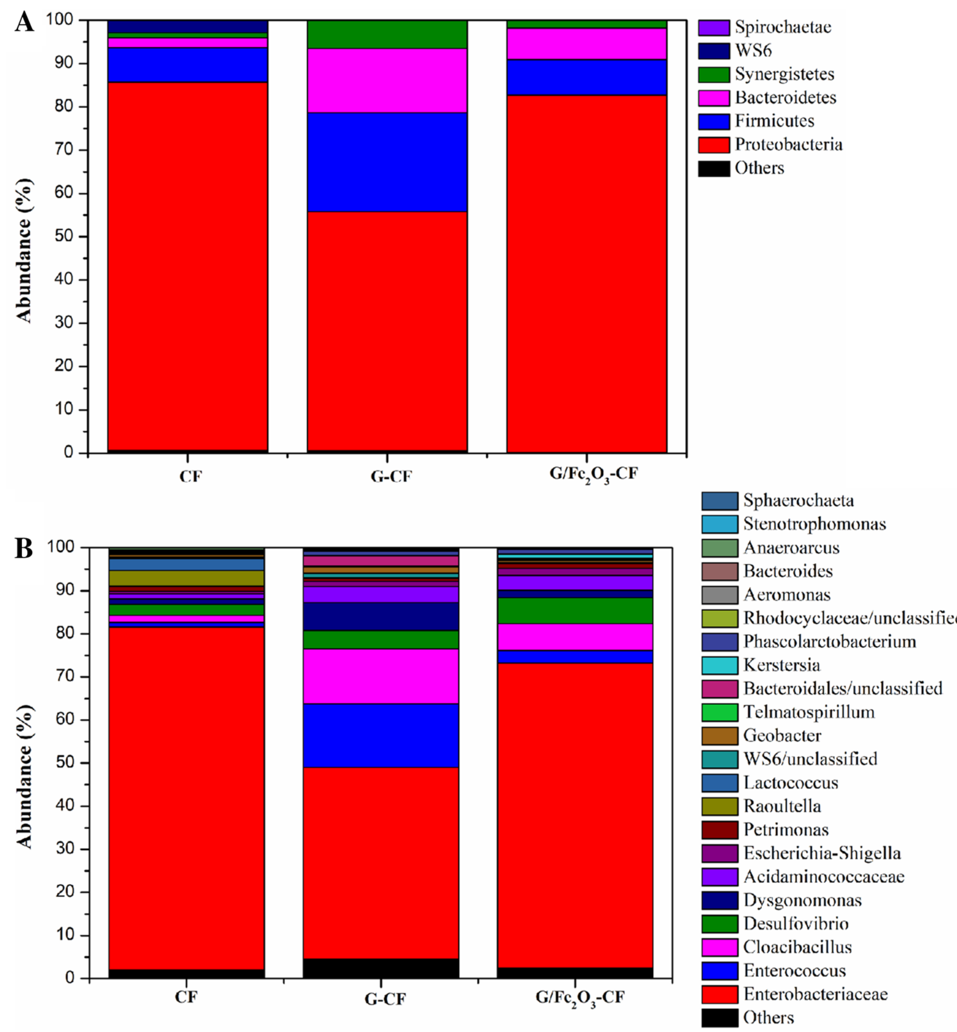

Fig. 8 Relative abundance of bacterial phylum level (**a**) and genus level (**b**) in biofilms with CF, G-CF and G/Fe_2O_3-CF at the end of the experiment

Proteobacteria in CF (85.1%) and G/Fe_2O_3–CF (82.6%) were significantly higher than that in G–CF (55.3%), and the relative abundances of Firmicutes and Bacteroidetes in G–CF were higher than the others. Microbial communities were also identified at the genus level (Fig. 8b). The main genus included *Enterobacteriaceae*, *Enterococcus*, *Cloacibacillus* and *Desulfovibrio*. Among them, *Enterobacteriaceae* had the highest relative abundance, and the members of this genus are exoelectrogenic bacteria with the ability to transfer electrons to the electrodes [28]. The relative abundances of

Enterobacteriaceae was 79.6% in CF, while its abundance was only 44.5% in G-CF group. These results were similar to those observed in a previous study [29], which found that the proportion of *Geobacter* (well-known exoelectrogenic bacteria) in G–CF was lower than that in the control in MFCs. The hydrophobicity of graphene [30] reduced its affinity to bacterial attachment and affected the enrichment of exoelectrogens. However, the relative abundance of *Enterobacteriaceae* in G/Fe_2O_3–CF (70.8%) was slightly lower than that in the CF group but was significantly higher than that in the G–CF group. This phenomenon might be due to the good biocompatibility of Fe_2O_3 that contributed to stimulating the activity of iron-reducing bacteria, which were mainly exoelectrogens [31, 32]. *Enterococcus* and *Cloacibacillus* maintained a higher abundance in the G-CF than the others. Different from the exoelectrogens, *Enterococcus* and *Cloacibacillus* belonged to fermentation bacteria, which could use sugar to produce small molecular organic acids [33, 34]. Exoelectrogens may further utilize these organic acids to generate electricity. The introduction of graphene mainly provided high electrical conductivity to facilitate EET. The relative abundance of *Desulfovibrio* in the G/Fe_2O_3–CF (6.3%) group was significantly higher than that in the CF (2.6%) and G–CF (4.2%) groups. *Desulfovibrio* has been reported to be cable bacteria [35], which was filamentous bacteria that transport electrons across distances of several centimeters and connect spatially separated electron donors and acceptors [36]. Notably, the semiconductor properties of Fe_2O_3 are favorable to long-distance EET [37]. Therefore, the semiconductive iron oxides in G/Fe_2O_3–CF likely acted as electron conduits between bacterial cells and distant electron acceptors such as the electrodes and then provided adequate conditions for *Desulfovibrio* growth during the electricity generation.

MFC anodes can be modified using graphene-based materials with or without binders. The main binders are polymeric materials and metal oxide materials. PANI is a polymer commonly used to functionalize anodes [38]. The remarkable enhancement in MFC might be ascribed to the high electrical conductivity of graphene and the large surface of PANI. More importantly, PANI carries a positive charge in a neutral environment, which favors the adhesion growth of negatively charged bacteria and enhances biocompatibility [39]. Metal oxides are mainly semiconductors and their composites are applied to the anode modification of MFCs [40]. Among several metal oxide semiconductors, TiO_2 and SnO_2 have been widely explored because of their unique chemical sensitivity and conductivity. In addition, semiconductors are also nontoxic, chemically stable and biocompatible [41, 42].

In our study, a novel anode material of G/Fe_2O_3 composite was designed. The power density of the MFC with G/Fe_2O_3 was lower than that described in several studies [38, 39, 43] possibly because of our higher reactor volume and the absence of Pt as a cathodic catalyst in our study. We also noticed that the abundance of *Geobacter* was significantly lower than that reported in a previous work [43] because we used different inoculation sources. However, the power density of MFC with the G/Fe_2O_3 was 2.59 times that of the control, which was higher than that of MFC with the soluble Fe (III) with pure culture (2.13 times [16]) or mixed culture (1.23 times [43]). This result showed that graphene-enhanced the poor conductivity of Fe_2O_3 in MFCs. Moreover, the electrode decorated with G/Fe_2O_3 could be reused through a simple one-step hydrothermal reduction, and the process of repeated addition of soluble ferric iron could be reduced to improve the MFC performance. In addition, the enhancement mechanism of the MFC with G/Fe_2O_3 was different from that of previously reported MFCs. In the MFC containing *S. oneidensis*, the release of flavin as an electron shuttle can be promoted by the addition of Fe (III) for electron transfer [16]. The addition of soluble Fe (III) to the mixed culture also increases the abundance of *Geobacter* on the anode biofilm, thereby improving the performance of the MFCs [43]. However, in our study, G/Fe_2O_3 can promote the abundance of *Desulfovibrio* and enhance electron transport efficiency over long distances. These effects may be due to the synergy between the excellent electronic conductivity of graphene and the good biocompatibility of ferric oxide. They are also beneficial to the enhancement of electron transfer in MFC systems.

Conclusion

In this research, we used a simple one-step hydrothermal reduction method to prepare G/Fe_2O_3-CF. The G/Fe_2O_3-CF can effectively increase the voltage and output power of the MFC and reduce the internal resistance of the entire MFC system. The P_{max} of G/Fe_2O_3-CF was 334 ± 4 mW/m^2, which was 1.72 times and 2.59 times that of G-CF and CF, respectively. The internal resistance of G/Fe_2O_3-CF was the lowest (320 ± 5 Ω). Illumina high-throughput sequencing results showed that microbial communities varied with different electrodes. The majority of the predominant populations on the anode biofilm were affiliated with *Enterobacteriaceae*, the abundance of the *Desulfovibrio* was enhanced in the MFC with G/Fe_2O_3-CF.

Acknowledgments This work was supported by the National Key Research and Development Program of China (2018YFA0901300), the National Natural Science Foundation of China (Grant No.: 21878150); the Key projects of modern agriculture in Jiangsu Province (Grant No.: BE2018394); Fund from the State Key Laboratory of Materials-Oriented Chemical Engineering (ZK201605) and the Jiangsu Synergetic Innovation Center for Advanced Bio-Manufacture.

Compliance with ethical standards

Conflict of interest The authors declare that they have no conflict of interest.

References

1. Kakarla R, Min B (2014) Photoautotrophic microalgae scenedesmus obliquus attached on a cathode as oxygen producers for microbial fuel cell (MFC) operation. Int J Hydrog Energy 39:10275–10283
2. Logan BE (2009) Exoelectrogenic bacteria that power microbial fuel cells. Nat Rev Microbiol 7:375–381
3. Wang HY, Wang GM, Ling YC, Qian F, Song Y, Lu XH, Chen SW, Tong YX, Li Y (2013) High power density microbial fuel cell with flexible 3D graphene-nickel foam as anode. RSC 5:10283–10290
4. Juang DF, Yang PC, Chou HY, Chiu LJ (2011) Effects of microbial species, organic loading and substrate degradation rate on the power generation capability of microbial fuel cells. Biotechnol Lett 33:2147–2160
5. Logan BE, Hamelers B, Rozendal R, Schröder U, Keller J, Freguia S, Aeltermann P, Varstraete W, Rabaey K (2006) Microbial Fuel Cells: Methodology and Technology. Environ Sci Technol 40:5181–5192
6. Mehdinia A, Ziaei E, Jabbari A (2014) Multi-walled carbon nanotube/SnO_2 nanocomposite: a novel anode material for microbial fuel cells. Electrochim Acta 130:512–518
7. Santoro C, Guilizzoni M, Baena JP, Pasaogullari U, Casalegno A, Li B, Babanova S, Artyushkova K, Atanassov P (2014) The effects of carbon electrode surface properties on bacteria attachment and start up time of microbial fuel cells. Carbon 67:128–139
8. Yu YY, Yong YC, Guo CX, Song H, Li CM (2014) Nitrogen doped carbon nanoparticles enhanced extracellular electron transfer for high-performance microbial fuel cells anode. Chemosphere 140:26–33
9. Reshetenko TV, Kim HT, Krewer U, Kweon HJ (2007) The effect of the anode loading and method of MEA fabrication on DMFC performance. Fuel Cells 7:238–245
10. Stankovich S, Dikin DA, Dommett GHB, Kohlhaas KM, Zimney EJ, Stach EA, Piner RD, Nguyen SBT, Ruoff RS (2006) Graphene-based composite materials. Nature 442:282–286
11. Li D, Müller MB, Gilje S, Kaner RB, Wallace GG (2008) Processable aqueous dispersions of graphene nanosheets. Nat. Nanotechnol 3:101–105
12. Xiao L, Damien J, Luo JY, Jang HD, Huang JX, He Z (2012) Crumpled graphene particles for microbial fuel cell electrodes. J Power Sour 208:187–192
13. Wang Y, Zhao C, Sun D, Zhang JR, Zhu JJ (2013) Graphene/poly (3,4-ethylenedioxy-thiophene) hybrid as an anode for high-performance microbial fuel cells. ChemPlusChem 78:823–829
14. Kerisit S, Rosso KM, Dupuis M, Valiev M (2007) Molecular computational investigation of electron-transfer kinetics across cytochrome-Iron oxide interfaces. J Phys Chem C 111:11363–11375
15. Lower BH, Shi L, Yongsunthon R, Droubay TC, McCready DE, Lower SK (2007) Specific bonds between an iron oxide surface and outer membrane cytochromes MtrC and OmcA from *Shewanella oneidensis* MR-1. J Bacteriol 189:4944–4952
16. Wu D, Xing D, Lu L, Wei M, Liu B, Ren N (2013) Ferric iron enhances electricity generation by *Shewanella oneidensis* MR-1 in MFCs. Bioresour Technol 135:630–634
17. Beliaev AS, Saffarini DA, Mc Laughlin JL, Hunnicutt D (2001) MtrC, an outer membrane decahaem c cytochrome required for metal reduction in *Shewanella putrefaciens* MR-1. Mol Microbiol 39:722–730
18. Xiong Y, Shi L, Chen B, Mayer MU, Lower BH, Londer Y (2006) High-affinity binding and direct electron transfer to solid metals by the *Shewanella oneidensis* MR-1 Outer membrane c-type cytochrome OmcA. J Am Chem Soc 128:13978–13979
19. Jin YC, Qian J, Wang K, Yang XW, Dong XY, Qiu BJ (2013) Fabrication of multifunctional magnetic FePc@Fe_3O_4/reduced graphene oxide nanocomposites as biomimetic catalysts for organic peroxide sensing. J Electroanal Chem 693:79–85
20. Song TS, Cai HY, Yan ZS, Zhao ZW, Jiang HL (2012) Various voltage productions by microbial fuel cells with sedimentary inocula taken from different sites in one freshwater lake. Bioresour Technol 108:68–75
21. Tamura H, Goto K, Yotsuyanagi T, Nagayama M (1974) Spectrophotometric determination of iron (II) with 1,10-phenanthroline in the presence of large amounts of iron (III). Talanta 21:314–318
22. Song TS, Yan ZS, Zhao ZW, Jiang HL (2010) Removal of organic matter in freshwater sediment by microbial fuel cells at various external resistances. J Chem Technol Biotechnol 85:1489–1493
23. Moon IK, Lee J, Ruoff RS, Lee H (2010) Reduced graphene oxide by chemical graphitization. Nat Commun 1:73
24. Ferrar AC (2007) Raman spectroscopy of graphene and graphite: disorder, electron–phonon coupling, doping and nonadiabatic effects. Soild State Commun 143:47–57
25. Li S, Hu YY, Xu Q, Sun Z, Hou B, Zhang YP (2012) Iron and nitrogen-functionalized graphene as a non-precious metal catalyst for enhanced oxygen reduction in an air-cathode microbial fuel cell. J Power Sour 213:265–269
26. Song TS, Tan WM, Xie JJ (2018) Bio-reduction of graphene oxide using sulfate-reducing bacteria and its implication on anti-biocorrosion. J Nanosci Nanotechno 18:1–7
27. Greene AC, Patel BKC, Sheehy AJ (1997) *Deferribacter thermophilus* gen. nov., sp. nov., a novel thermophilic manganese and iron-reducing bacterium isolated from a petroleum reservoir. Int J Syst Bacteriol 47:505–509
28. Rabaey K, Lissens G, Siciliano SD, Verstraete W (2003) A microbial fuel cell capable of converting glucose to electricity at high rate and efficiency. Biotechnol Lett 25:1531–1535
29. Yoshida N, Miyata Y, Mugita A, Iida K (2016) Electricity recovery from municipal sewage wastewater using a hydrogel complex composed of microbially reduced graphene oxide and sludge. Materials (Basel) 9:742
30. Leenaerts O, Partoens B, Peeters FM (2009) Water on graphene: Hydrophobicity and dipole moment using density functional theory. Phys Rev B 79:235440
31. Logan BE, Regan JM (2006) Electricity-producing bacterial communities in microbial fuel cells. Trends Microbiol 14:512–518
32. Lovley DR (2006) Bug juice: harvesting electricity with microorganisms. Nat Rev Microbiol 4:497–508
33. Franz CMAP, Van Belkum MJ, Holzapfel WH, Abriouel H, Gálvez A (2007) Diversity of enterococcal bacteriocins and their grouping in a new classification scheme. FEMS Microbiol Rev 31:293–310
34. Ganesan A, Chaussonnerie S, Tarrade A, Dauga C, Bouchez T, Pelletier E, Le Paslier D, Sghir A (2008) *Cloacibacillus evryensis gen*. nov., sp. nov., a novel asaccharolytic, mesophilic, amino-acid-degrading bacterium within the phylum “Synergistetes”, isolated from an anaerobic sludge digester. Int J Syst Evol Microbiol 59:2003–2012
35. Holmes DE, Bond DR, O’Neil RA, Reimers CE, Tender LR, Lovley DR (2004) Microbial communities associated with electrodes harvesting electricity from a variety of aquatic sediments. Microb Ecol 48:178–190

36. Pfeffer C, Larsen S, Song J, Dong M, Besenbacher F, Meyer RL, Kjeldsen KU, Schreiber L, Gorby YA, El Naggar MY, Leung KM, Schramm A, Petersen N, Nielsen LP (2012) Filamentous bacteria transport electrons over centimetre distances. Nature 491:218–221
37. Roden EE, Urrutia MM (2002) Influence of biogenic Fe (II) on bacterial crystalline Fe (III) oxide reduction. Geomicrobiol J 19:209–251
38. Hou J, Liu Z, Zhang P (2013) A new method for fabrication of graphene/polyaniline nanocomplex modified microbial fuel cell anodes. J Power Sour 224:139–144
39. Huang LH, Li XF, Ren YP, Wang XH (2016) In-situ modified carbon cloth with polyaniline/graphene as anode to enhance performance of microbial fuel cell. Int J Hydrog Energy 41:11369–11379
40. Benetton XD, Navarro-Ávila SG, Figueiras C (2010) Electrochemical evaluation of Ti/TiO_2-polyaniline anodes for microbial fuel cells using hypersaline microbial consortia for synthetic wastewater treatment. J New Mater Electrochem Syst 13:1–6
41. Wen Z, Ci S, Mao S, Cui S, Lu G, Yu K (2013) TiO_2 nanoparticles-decorated carbon nanotubes for significantly improved bioelectricity generation in microbial fuel cells. J Power Sour 234:100–106
42. Mehdinia A, Ziaei E, Jabbari A (2014) Facile microwave-assisted synthesized reduced graphene oxide/tin oxide nanocomposite and using as anode material of microbial fuel cell to improve power generation. Int J Hydrog Energy 39:10724–10730
43. Liu Q, Yang Y, Mei X, Liu B, Chen C, Xing D (2018) Response of the microbial community structure of biofilms to ferric iron in microbial fuel cells. Sci Total Environ 631–632:695–701